

Decays of  $^{101}\text{Rh}^m$  and  $^{101}\text{Rh}^g$ 

V. R. Vanin, A. Passaro, and A. M. P. Passaro

*Instituto de Física, Universidade de São Paulo, 01000 São Paulo, Brasil*

(Received 30 April 1985)

The decays of  $^{101}\text{Rh}^m$  and  $^{101}\text{Rh}^g$  nuclides were studied by gamma-ray spectroscopy using both singles and coincidence spectra. The sources were obtained with the  $^{103}\text{Rh}(\gamma,2n)^{101}\text{Rh}^{m,g}$  reaction. Six transitions earlier attributed to the decays of these nuclides were not confirmed. The energies (keV) and the relative intensities for the observed gamma transitions following the  $^{101}\text{Rh}^m$  decay are, respectively, 127.226(9), 0.79(2); 157.41(4), 0.280(5); 179.636(15), 0.660(15); 184.11(5), 0.193(3); 233.74(4), 0.2198(15); 238.27(4), 0.2505(17); 306.857(5), 100; 311.367(19), 0.0175(9); 417.86(5), 0.005; 545.117(7), 5.3(3). The energies and the relative intensities of the gamma transitions observed for the  $^{101}\text{Rh}^g$  decay are the following: 110.94(12), 0.06(2); 127.226(9), 93.2(9); 184.22(13), 0.081(14); 198.01(3), 100; 295.01(3), 0.815(24); 325.23(3), 16.20(15); 422.19(8), 0.272(15). This work shows that only six excited levels are necessary to fit the observed data. Due to the simplification of the level scheme obtained in this work, the nuclear structure of the  $^{101}\text{Ru}$  for low excitation energy can be described qualitatively with a quasi-particle-phonon model.

## I. INTRODUCTION

The  $^{101}\text{Ru}$  nucleus has been the subject of extensive experimental investigation in the last decades. There are measurements of spectroscopic factors in particle transfer reactions,<sup>1,2</sup> electric quadrupole transition probabilities by Coulomb excitation,<sup>3</sup> half-lives of several levels in different experiments,<sup>4-6</sup> static magnetic dipole and quadrupole moments,<sup>7-9</sup> gamma and beta spectroscopy of the parent nuclei  $^{101}\text{Rh}$  and  $^{101}\text{Tc}$  (Refs. 10-16), and on-line gamma spectroscopy.<sup>17-19</sup> Harmatz<sup>20</sup> reviewed the data up to 1979.

The latest study of the decays of  $^{101}\text{Rh}^m$  and  $^{101}\text{Rh}^g$  to  $^{101}\text{Ru}$  was made by Sieniawski *et al.*<sup>13</sup> (Hereafter, reference to the work of Sieniawski, Petterson, and Nyman<sup>13</sup> will be abbreviated as SPN.) Some of the levels which they attributed to  $^{101}\text{Ru}$  were observed neither in the  $^{101}\text{Tc}$   $\beta^-$  decay<sup>20</sup> nor in the other experiments quoted above. It is not possible, however, to disclaim the existence of these levels only because they are not observed in other experiments, since the other experiments are selective in some sense. Also, it is not easy to follow the systematic trends of the excited levels in odd Ru isotopes, since the level densities vary quite strongly with mass number. The previous  $^{101}\text{Rh}^{m,g}$  decay studies can be verified, therefore, only by repeating them.

In this work, we shall report our measurements of the  $^{101}\text{Rh}^{m,g}$  decays with strong, though mixed, sources. Biparametric data were taken in the coincidence experiment and we attained high counting statistics both in the coincidence and in the singles spectra. Statistical techniques for defining upper intensity limits for unobserved gamma transitions allowed a quantitative description of the incompatibilities of our results with previous work.

## II. EXPERIMENTAL METHOD

## A. Source preparation

Natural metallic rhodium (0.6 g) was irradiated in the bremsstrahlung beam of the linear accelerator of the Insti-

tuto de Física da Universidade de São Paulo. One run, with 26 MeV electrons and 0.7  $\mu\text{A}$  current during 165 h, yielded the 0.19 g/cm<sup>2</sup> source for the  $^{101}\text{Rh}^g$  ( $T_{1/2}=3.3$  yr) decay measurements. Another run, with 31 MeV electrons and 0.8  $\mu\text{A}$  current during 35 h, yielded both the 0.45 g, 0.21 g/cm<sup>2</sup> source for the decay measurements of  $^{101}\text{Rh}^m$  ( $T_{1/2}=4.34$  d) and the 30 mg/cm<sup>2</sup>, 0.10 g total, source for the coincidence measurements.

## B. Detection systems

The singles spectra were taken with either a coaxial Ge(Li) detector of 80 cm<sup>3</sup> active volume or a coaxial HPGe detector of 104 cm<sup>3</sup> active volume. Both detectors gave 1.05 and 1.53 keV resolution for the 127 and 628 keV  $\gamma$  rays, respectively, during the measurements. The amplifier (Ortec 572) was used in the pileup rejection mode. The smaller detector was shielded with a lead cylinder which transmitted about 9% and 18% of the 238 and 609 keV lines of the room background, respectively. The larger detector was shielded with an iron cylinder 10 cm thick which transmitted about 1% and 2% for the same background lines. Four annular lead pieces were put into the iron shield, between source and detector, to absorb photons scattered by the low-Z shield without decreasing the effective solid angle.

The detectors utilized in the coincidence experiment were a coaxial Ge(Li) detector of 53 cm<sup>3</sup> active volume and a planar HPGe detector, with 5 cm<sup>3</sup>. By placing the detectors to form an angle of 90° between axes and by shielding each detector with 1 cm of lead, the coincidences due to Compton scattered gamma rays between detectors were greatly reduced. The fast-slow coincidence circuit is conventional, with rejection of slow rise time pulses in the 53 cm<sup>3</sup> detector in the fast coincidence and pileup rejection in the slow coincidence. The time resolution (FWHM) was 8 ns and the full width at one-tenth maximum, 20 ns. Two time windows of 30 ns width separated by 70 ns were used, one for true plus chance coincidence and the other for chance coincidence only.

The three parameters—energies in both detectors and time window—were simultaneously recorded on magnetic tape for later analysis.

### III. MEASUREMENTS AND RESULTS

#### A. $^{101}\text{Rh}^m$

The  $^{101}\text{Rh}^m$  gamma decay spectrum was measured with the  $80\text{ cm}^3$  detector in 19 runs, totaling 133 h of live counting time over a period of ten days. The summed spectrum is shown in Fig. 1. The attribution of lines to  $^{101}\text{Rh}^m$  decay rely primarily on the associated lifetime. We obtained 4.36(1) d for the  $^{101}\text{Rh}^m$  lifetime, in close agreement with Aras *et al.*<sup>11</sup> However, we use the result of Aras *et al.* as our result may be subject to greater systematic errors.

The gamma transition energies were measured in simultaneous counting of the  $^{101}\text{Rh}^m$  source with  $^{152}\text{Eu}$ ,  $^{133}\text{Ba}$ , and  $^{137}\text{Cs}$  sources, except for the weak 311 and 418 keV gamma transitions for which the other  $^{101}\text{Rh}^m$  gamma

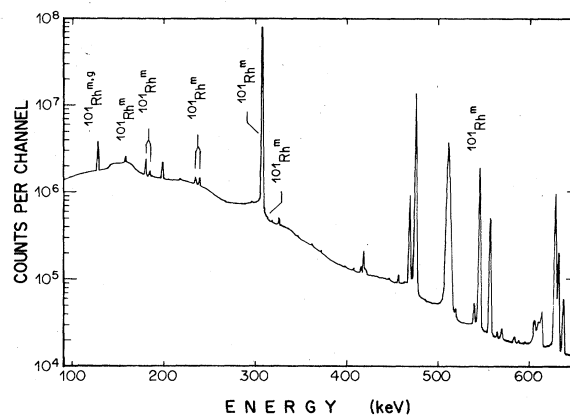


FIG. 1. Gamma-ray spectrum resulting from the sum of the spectra taken to follow the  $^{101}\text{Rh}^m$  activity. Unassigned lines were attributed to the decays of the competing activities due to the contaminants, to background lines, or to accidental summing in the detector. One channel in this spectrum corresponds to 0.185 keV.

TABLE I.  $^{101}\text{Rh}^m$   $\gamma$  ray energies ( $E_\gamma$ ) and relative intensities ( $I_\gamma$ ), adopted total internal conversion coefficients (ICC), and transition intensities per decay ( $I_t$ ).

$E_\gamma^a$ (keV)	This work <sup>b</sup>	$I_\gamma$ SPN	Adopted ICC <sup>c</sup>	$I_t$ (%)
4.5*				<0.002 <sup>d,e</sup>
127.226(9)	0.79(2)	0.65(2)	0.19(2) <sup>f</sup>	0.81(3)
157.41(4)	0.280(5)	0.29(2)	26.5 <sup>g</sup>	6.44(11)
179.636(15)	0.660(15)	0.56(2)	0.159 <sup>g</sup>	0.663(15)
184.11(5)	0.193(3)	0.155(10)	0.076(11) <sup>h</sup>	0.180(3)
233.74(4)	0.2198(15)	0.20(2)	0.031 <sup>g</sup>	0.1966(13)
238.27(4)	0.2505(17)	0.23(2)	0.030 <sup>g</sup>	0.2239(15)
306.857(5)	100	100	0.0156 <sup>g</sup>	88.1(3)
311.40(3)	0.0175(9)	0.04(1)	0.0150 <sup>g</sup>	0.0154(8)
332.5(2)*	<0.0017 <sup>d</sup>	0.032(6)		
337.0(3)*	<0.0024 <sup>d</sup>	0.039(7)		
417.86(5)	~0.005 <sup>e</sup>	0.022(10)	0.010 <sup>g</sup>	~0.004
489.0(5)*	<0.0021 <sup>d</sup>	~0.01		
496.0(5)*	<0.0017 <sup>d</sup>	0.015(3)		
545.117(7)	5.3(3)	4.6(2)	0.004 <sup>g</sup>	4.7(3)
616.5(7)*	<0.0017 <sup>i</sup>	~0.003		
623.8(7)*		0.012(3)		
643.5(8)*	<0.0008	~0.004		

<sup>a</sup>This work, except when marked by an asterisk (\*), indicating SPN.

<sup>b</sup>Corrected for self-absorption.

<sup>c</sup>The transition multiplicities are taken from Harmatz (Ref. 20) though some ICC are somewhat different. The adopted criteria for ICC are shown in each case.

<sup>d</sup>A line corresponding to an intensity greater than the value quoted has 95% probability of detection in our spectra but was not seen.

<sup>e</sup>Estimated from the coincidence experiment.

<sup>f</sup>Unweighted average from Refs. 13, and 22–24.

<sup>g</sup>Theoretical value (Ref. 25) for probable multiplicity.

<sup>h</sup>From SPN.

<sup>i</sup>We could not determine an upper intensity limit from our spectra. This value comes from the 489 and 616 keV transitions branching ratio determined by Kistner *et al.* (Ref. 3).

transitions were used as standards. The 418 keV transition was observed only in the coincidence measurement due to the presence of the 418.5 keV line in the competing activity,  $^{102}\text{Rh}^m$ .<sup>21</sup> The detector efficiency was calibrated with a  $^{152}\text{Eu}$  source. No correction for the extended  $^{101}\text{Rh}^m$  source geometry was needed, since the source-detector separation was 15 cm. Summing effects were taken in account only for the 311 and 418 keV gamma-ray intensity measurement.

Except for a weak 596 keV line observed only in the 133 h spectrum, all the lines observed were attributed to  $^{101}\text{Rh}^m$ , to competing activities caused by  $(\gamma,2n)$  and  $(\gamma,3n)$  reactions with  $^{103}\text{Rh}$  ( $^{102}\text{Rh}^m$ ,  $^{102}\text{Rh}^g$ ,  $^{101}\text{Rh}^g$ , and  $^{100}\text{Rh}$ ), activities due to contamination by Ir (100 ppm) and Sb (50 ppm) ( $^{190}\text{Ir}$ ,  $^{192}\text{Ir}$ , and  $^{122}\text{Sb}$ ), background radiation, and accidental summing in the detector.

Table I shows the gamma-ray energies and intensities, the latter compared with the results reported by SPN. Our upper limits for intensities of transitions observed by SPN were calculated with Helene's prescription<sup>26</sup> for a

95% confidence level. The upper limits of the 624 and 616 keV gamma intensities, previously observed by SPN, were not determined in this experiment due to the proximity of lines at 628 keV [ $^{102}\text{Rh}^m$  (Ref. 21)] and at 614 keV (accidental sum of two 307 keV gamma rays from  $^{101}\text{Rh}^m$  decay).

### B. $^{101}\text{Rh}^g$

The  $^{101}\text{Rh}^g$  decay was observed in three runs with the 104 cm<sup>3</sup> detector over a 200 d interval, except for the electron capture (EC) to the  $^{101}\text{Ru}$  ground state. The last of the spectra obtained is shown in Fig. 2. As the lifetime of the  $^{101}\text{Rh}^g$  ( $T_{1/2}=3.3$  yr) is very close to that of  $^{102}\text{Rh}^g$  ( $T_{1/2}=2.9$  yr), the attribution of a line to  $^{101}\text{Rh}^g$  cannot be based solely on the lifetime. The activities due to contaminants observed in the  $^{101}\text{Rh}^m$  decay study, however, are not observed in this case due to their smaller lifetime.

Table II shows gamma-ray energies and intensities, to-

TABLE II.  $^{101}\text{Rh}^g$  gamma ray energies ( $E_\gamma$ ) and relative intensities ( $I_\gamma$ ), adopted internal conversion coefficients (ICC), and total transition intensities per decay ( $I_t$ ).

$E_\gamma^a$ (keV)	This work <sup>b</sup>	$I_\gamma$	SPN <sup>c</sup>	Adopted ICC <sup>d</sup>	$I_t^e$ (%)
97.5(10)*	<0.18 <sup>f</sup>		~0.1		
110.94(12)	0.06(2)		~0.1	0.235 <sup>g</sup>	0.05(2)
114.5(3)*	<0.09 <sup>f</sup>		~0.1		
127.226(9)	93.2(9)		103	0.19(2) <sup>h</sup>	76(6)
137.6(5)*	<0.11 <sup>f</sup>		0.3(1)		
184.22(13)	0.081(14)		0.13(6)	0.076(11) <sup>i</sup>	0.06(1)
198.01(3)	100		100(2)	0.049(2) <sup>j</sup>	71(6)
217.0(3)*	k		0.87(16)		
295.01(3)	0.815(24)		1.0(3)	0.02 <sup>l</sup>	0.57(5)
306.8(1)*	<0.2 <sup>f</sup>		~0.08		
325.23(3)	16.20(15)		19.0(15)	0.020 <sup>m</sup>	11(1)
334.5(5)*	<0.18 <sup>f</sup>		0.10(5)		
344.0(4)*			0.30(10)		
422.19(8)	0.272		0.52(8)	0.007 <sup>n</sup>	0.19(2)
462.5(4)*	k		0.10(3)		

<sup>a</sup>This work, except when marked by an asterisk (\*), indicating SPN.

<sup>b</sup>Corrected for self-absorption.

<sup>c</sup>In the original work, the data were normalized to the 127 keV gamma transition.

<sup>d</sup>The transition multipolarities are taken from Harmatz (Ref. 20). The adopted criteria for ICC are shown in each case.

<sup>e</sup>The EC to the  $^{101}\text{Ru}$  ground state was measured as 13(7)% of the decays.

<sup>f</sup>A line corresponding to an intensity greater than the value quoted has 95% probability of detection in our spectra but was not seen.

<sup>g</sup>Theoretical value (Ref. 25) for  $M1$ .

<sup>h</sup>Unweighted average from Refs. 13, 22–24.

<sup>i</sup>From SPN.

<sup>j</sup>From the multipole mixing ratio measured by Wood *et al.* (Ref. 23) and theoretical conversion coefficients (Ref. 25).

<sup>k</sup>A line with an energy near that given in the first column was observed but attributed to a transition following  $^{102}\text{Rh}^m$  decay.

<sup>l</sup>Theoretical values (Ref. 25):  $M1$ , 0.0173;  $E2$ , 0.0285.

<sup>m</sup>Theoretical value (Ref. 25) for  $E2$ .

<sup>n</sup>Theoretical values (Ref. 25):  $M1$ , 0.007;  $E2$ , 0.009.

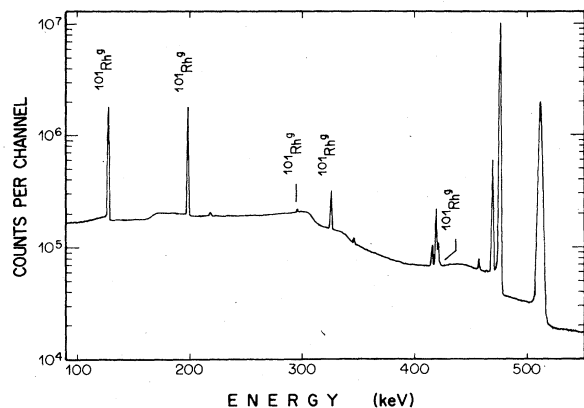


FIG. 2. Gamma-ray spectrum taken to follow  $^{101}\text{Rh}^g$  activity. Unassigned lines were attributed to the decays of  $^{102}\text{Rh}^m$  and  $^{102}\text{Rh}^g$  or are background lines. One channel in this spectrum corresponds to 0.193 keV.

gether with the intensities of SPN. Selected gamma transitions which follow  $^{102}\text{Rh}^{m,g}$  decays [345, 418, 475, 556, and 629 keV (Ref. 21)] and  $^{101}\text{Rh}^g$  decay (127 and 198 keV) were used as energy standards. The energies of the gamma transitions which follow  $^{102}\text{Rh}^{m,g}$  were taken from the compilation by Gelder *et al.*<sup>21</sup> The energies of the 127 and 198 keV gamma transitions were measured simultaneously with the energies of the gamma rays which follow  $^{101}\text{Rh}^m$  decay (see footnote a of Table I). Efficiency was calibrated with a  $^{152}\text{Eu}$  source. Upper intensity limits were calculated with Helene's prescription, except for the 344 keV gamma transition due to its proximity with the 346 keV gamma transition following  $^{102}\text{Rh}^g$  decay.<sup>21</sup> The 217 and 463 keV gamma rays were observed in the spectra but attributed to transitions following  $^{102}\text{Rh}^m$  decay through the coincidence measurement.

The EC to the  $^{101}\text{Ru}$  ground state was measured through the growth of the observed gamma activity following  $^{101}\text{Rh}^g$  decay due to the  $^{101}\text{Rh}^m$  isomeric transition (IT) feeding. The singles spectra taken for the  $^{101}\text{Rh}^m$  decay study were used for this measurement. This procedure is subject to large systematic errors due to eventual inaccuracy in the IT intensity, in the  $^{101}\text{Rh}^g$  half-life, and in the total transition intensities which follow  $^{101}\text{Rh}^g$  decay. We conclude that 13(7)% of the  $^{101}\text{Rh}^g$  decays proceed directly to  $^{101}\text{Ru}^g$ .

### C. Coincidence measurement

The counting time was 9.3 d. The data were acquired simultaneously with the singles spectra taken for the  $^{101}\text{Rh}^m$  decay study. The average chance to true coincidence was 5%. The spectrum of coincidences with the 307 keV gamma ray is shown in Fig. 3, uncorrected for chance coincidences or Compton scattered events. These corrections were performed in one of the following ways: (1) with appropriate spectra analyzed separately; (2) summing the chance spectrum with the appropriately generated spectrum of Compton scattered events and subsequently subtracting this from the spectrum of "true" coin-

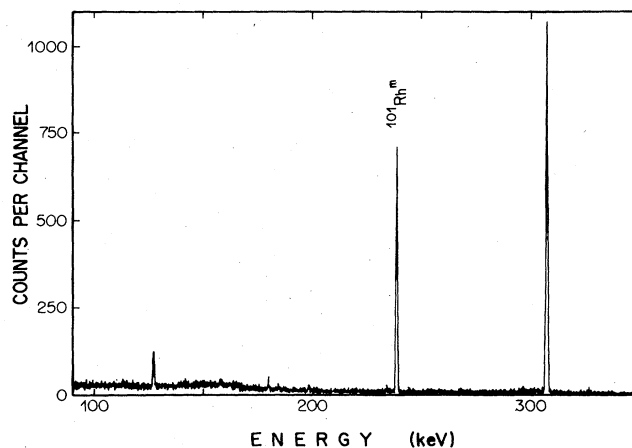


FIG. 3. Gamma-ray spectrum taken in coincidence with the 307 keV gamma rays ( $^{101}\text{Rh}^m$ ). Unassigned lines are due to chance coincidences or coincidences with Compton scattered photons. One channel in this spectrum corresponds to 0.0883 keV.

cidences. In case 2, the variances in the countings in each channel of the subtracted spectrum were taken as the sum of the countings of the chance, Compton, and true spectra.<sup>27</sup> Table III summarizes the coincidence measurements. Sum peaks are not shown in Table III. Identification of sum peaks with Ru K x rays is quite important since a very small line at 217.0 keV was observed in coincidence with the 127 keV gamma rays. The intensity of this coincidence, however, could be completely attributed to the coincidence of the 127 keV gamma rays with the 198 + Ru  $K_\alpha$  sum peak by comparison with several other coincidences with Ru K x-ray sum peaks.

From the results we can attribute both the 217.7 and the 462.7 keV gamma rays to  $^{102}\text{Rh}^m$  or  $^{102}\text{Rh}^g$  decays. It is known that the 217.7 keV transition follows only the decay of  $^{102}\text{Rh}^m$  (Ref. 21) which implies that the 462.7 keV transition also follows  $^{102}\text{Rh}^m$  decay. We point out

TABLE III. Summary of the coincidences. The nuclide to which we ascribed the coincidences is shown in the second column. Energy gate widths are less than 2 keV.

Gate (keV)	Radioisotope	Gammas in coincidence energies in keV
127	$^{101}\text{Rh}^{m,g}$	179.66, 184.17, 197.99, 233.75, 238.1, 294.90, 417.86
180	$^{101}\text{Rh}^m$	127.25, 238.1
184	$^{101}\text{Rh}^m$	127.24, 233.76
198	$^{101}\text{Rh}^g$	127.19
218	$^{102}\text{Rh}^m$	462.7, 475.1
234	$^{101}\text{Rh}^m$	127.2, 184.17, 311.41
238	$^{101}\text{Rh}^m$	127.3, 179.7, 306.84
307	$^{101}\text{Rh}^m$	238.23
311	$^{101}\text{Rh}^m$	233.72
475	$^{102}\text{Rh}^m$	217.6
545	$^{101}\text{Rh}^m$	none

that the 217.7-462.7 keV transition cascade could not occur in  $^{101}\text{Rh}^g$  decay since the EC energy available is only 541(17) keV.<sup>20</sup>

Due to the large (40%) and probably inaccurate correction for peak summing in the determination of the 418 keV gamma intensity from this coincidence measurement, we do not quote errors for this result. Finally, we point out that all coincidences implied by the proposed decay scheme of  $^{101}\text{Rh}^m$  were directly measured in this experiment.

#### D. Possible sources of disagreement

The 218 and 463 keV gamma transitions can be attributed to  $^{102}\text{Rh}^m$  activity in SPN's source. The 332, 335, and 337 keV gamma transitions could be assigned as the Compton edge of the 511 keV annihilation gamma rays from the  $^{102}\text{Rh}^m$  decay. The 344 keV gamma transition may be the 346 keV gamma ray which follows  $^{102}\text{Rh}^g$  decay.

The 234-307 keV coincidences can be attributed to absorption of about 307 keV of energy of a 545 keV photon in one detector, the scattered photon being detected by the other detector in absence of proper shielding. This would result in the broad peak observed by SPN, as other broad peaks appearing in their coincidence spectra suggest this hypothesis.

### IV. DECAY SCHEME

Combining our results with the internal conversion coefficients of Tables I and II, the decay schemes of  $^{101}\text{Rh}^{m,g}$  were established and are shown in Fig. 4. Spins,

parities, and EC available energy are taken from Harmatz<sup>20</sup> except where noted.

All the lines attributed to  $^{101}\text{Rh}^m$  and  $^{101}\text{Rh}^g$  decays were included in the schemes. There are four levels less than in the scheme proposed by SPN. One of the levels has a different spin assignment than that given by SPN. We discuss the changes below.

#### A. Level at 643.5 keV

None of the gamma transitions observed by SPN deexciting this level, with energies 332.0, 337.5, and 643.5 keV, were observed in this work. The intensities of the 332.0 and 337.5 keV gamma transitions proposed by SPN are greater than our upper limit by five standard deviations showing that the data from this work and from SPN are completely incompatible. In no other experiment is a level observed in  $^{101}\text{Ru}$  with about 643 keV energy excitation.<sup>1-3,5,6,10-12,14-19,22</sup>

#### B. Level at 624 keV

The 496 keV gamma transition attributed by SPN to the decay of this level was not observed in this work. The intensity proposed by SPN for this line is four standard deviations greater than our upper limit, therefore also showing incompatibility. The 624 keV transition was not observed in this work but we were unable to determine a reliable upper limit (see Sec. III). Also the experimental data on  $^{101}\text{Tc}$  beta decay reveal neither a  $^{101}\text{Ru}$  level at this energy nor 496 and 624 keV gamma transitions.<sup>12,14-16</sup> Comparing the beta decay of  $^{101}\text{Tc}$  with the beta decay of  $^{101}\text{Rh}^m$  we would expect that the feeding of

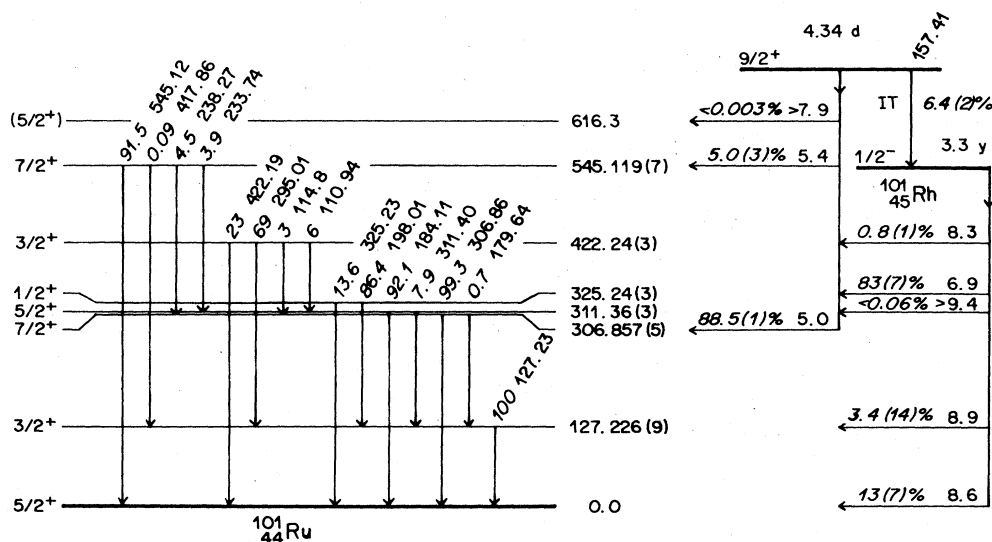


FIG. 4. Decay schemes of  $^{101}\text{Rh}^m$  and  $^{101}\text{Rh}^g$ , mainly from this work. Values of  $\log ft$  were calculated with the tables of Gove and Martin (Ref. 28). Upper intensity limits for electron capture are calculated at the 95% confidence level. The spins are taken from the compilation by Harmatz, except for the probable spin of the 616.3 keV level which was taken from Kajrys *et al.* (Ref. 19). The branching ratio between the 295 and 115 keV transitions was taken from Kistner *et al.* (Ref. 3).

the hypothetical 624 keV level would be stronger for  $^{101}\text{Tc}$ . Kistner and Schwarzschild<sup>3</sup> and Erokhina *et al.*<sup>5</sup> observe a level at 623.5 keV in  $^{101}\text{Ru}$  by Coulomb excitation. Hollas *et al.*<sup>1</sup> and Duarte<sup>2</sup> observe a level with about 624 keV in the  $^{100}\text{Ru}(\text{d,p})^{101}\text{Ru}$  transfer reaction with  $L=0$  angular momentum transfer and spectroscopic factor about 0.1. This reaction datum shows conclusively that they observe a  $\frac{1}{2}^+$  level, a conclusion that is not in contradiction with the Coulomb excitation datum, though the levels observed in the two experiments may not be the same. A  $\frac{1}{2}^+$  spin level would be fed by  $^{101}\text{Rh}^m$ —or  $^{101}\text{Tc}$ —by a fourth forbidden beta transition, surely many orders of magnitude slower than the allowed beta transitions observed in both decays. Concluding, most probably there is only one level with energy about 623.5 keV and with  $\frac{1}{2}^+$  spin.

#### C. Level at 616 keV

The 489 keV gamma transition was not observed in this work. Our upper intensity limit is equal to one-fifth the intensity observed by SPN. The ground state transition was not observed but we could not determine a reliable upper limit (see Sec. III). In the  $^{101}\text{Tc}$  decay measurements, Aras *et al.*<sup>12</sup> and Cook and Johns<sup>14,15</sup> observed these transitions, later disclaimed by Wright *et al.*<sup>16</sup> In the Coulomb excitation experiments (3,5), a level in  $^{101}\text{Ru}$  at 616 keV is observed with spin in the range  $\frac{1}{2}$  and  $\frac{3}{2}$  and positive parity. In a recent on-line gamma spectroscopy experiment, Kajrys *et al.*<sup>19</sup> observe a level at 616.3 keV with spin probably  $\frac{5}{2}^+$ , decaying by gamma transitions of 489 and 616 keV. The  $^{101}\text{Rh}^m$  decay to this level, if  $\frac{5}{2}^+$  is the true spin, would be very weak. Taking the 616/489 keV branching ratio determined by Kistner *et al.*<sup>3</sup> we calculated the upper limit for the feeding of this level by  $^{101}\text{Rh}^m$ . Concluding, in other experiments a level is observed at this energy in  $^{101}\text{Ru}$ . Our experiment is compatible with the  $\frac{5}{2}^+$  spin assignment by Kajrys *et al.*<sup>19</sup>

#### D. Level at 463 keV

SPN observed a 138 keV gamma transition deexciting this level. Our upper intensity limit for this transition is one-third that observed by SPN. The 463 keV gamma transition was observed in this work but assigned to  $^{102}\text{Rh}^m$  by our coincidence experiment (see Sec III). There is no evidence for a level with this energy in  $^{101}\text{Ru}$  in any other experiment.<sup>1-3,5,6,10-12,14-19,22</sup> Hence, the only remaining indication for the existence of this level is the weak 335 keV gamma transition observed by SPN, which we discard as arising from a Compton edge in the detector.

#### E. Level at 344 keV

The 217 keV gamma transition attributed by SPN as deexciting this level was assigned, in this work, to the decay of  $^{102}\text{Rh}^m$  (See Sec. III). Moreover, the 217-127 keV

cascade was not observed. There is no evidence for a level with this energy in  $^{101}\text{Ru}$  in any other experiment.<sup>1-3,5,6,10-12,14-19,22</sup> We note that although Kajrys *et al.*<sup>19</sup> expected to observe this level in their experiment the result was negative. The only remaining indication for the existence of this level, therefore, is given by the 344 keV gamma transition observed by SPN which we discard, assigning it as the 346 keV gamma transition following  $^{102}\text{Rh}^m$  decay.

#### F. Main disagreements in transition intensities: $^{101}\text{Rh}^m$

The 311 and 418 keV gamma transition intensities measured in this work are one-half and one-fifth the values of SPN, respectively. The branching ratio of the 311 and 184 keV transitions deexciting the 311 keV level in  $^{101}\text{Ru}$  determined in this work is in good agreement with Wright *et al.*<sup>16</sup> following the  $^{101}\text{Tc}$  decay. Wright *et al.* did not observe the 418 keV gamma ray transition in agreement with the measurement of a very small intensity for this line in our work. The branching ratio of the 418 and 545 keV transitions deexciting the 545 keV level determined by SPN would imply that, in the  $^{101}\text{Tc}$  beta decay, the intensity of the 418 keV gamma transition would be one-half the intensity of the well known 422 keV gamma transition.<sup>20</sup> We determined from our coincidence experiment an upper intensity limit for the 4.5 keV transition in  $^{101}\text{Ru}$  equal to one-fortieth the intensity given by SPN.

TABLE IV. Known  $^{101}\text{Ru}$  positive parity level energies ( $E$ ) and spins ( $I^\pi$ ) up to an excitation energy of 720 keV (Refs. 20, 2, 19, and this work), spectroscopic factors  $S$  measured in the  $^{100}\text{Ru}(\text{d,p})^{101}\text{Ru}$  reaction (Ref. 2), and assigned quantum numbers  $J$  (intrinsic state angular momentum),  $n$  (phonon number), and  $R$  (core angular momentum).

$E$ (keV)	$I^\pi$	$S^a$	$J$	$n$	$R$
0	$\frac{5}{2}^+$	2.08	$\frac{5}{2}$	0	0
127	$\frac{3}{2}^+$	0.069	$\frac{5}{2}$	1	2
307	$\frac{7}{2}^+$	4.73	$\frac{7}{2}$	0	0
311	$\frac{5}{2}^+$	<0.03	$\frac{5}{2}$	1	2
325	$\frac{1}{2}^+$	1.00	$\frac{1}{2}$	0	0
422	$\frac{3}{2}^+$	0.15			
531	$\frac{5}{2}^+; \frac{3}{2}^+$	0.72; 0.75			
545	$\frac{7}{2}^+$	n.obs.	$\frac{5}{2}$	1	2
598	$(\frac{3}{2}^+)$	n.obs.			
616	$(\frac{5}{2}^+)$	n.obs.			
623	$\frac{1}{2}^+$	0.06	$\frac{5}{2}$	1	2
685	$\frac{5}{2}^+; \frac{3}{2}^+$	0.15; 0.17			
720	$\frac{9}{2}^+$	n.obs.	$\frac{5}{2}$	1	2

<sup>a</sup>n.obs. stands for not observed. Also the 311 keV level was not observed in the transfer reaction, but in that case it was possible to define an upper limit for the spectroscopic factor (Ref. 2).

G. Main disagreements in  
gamma transition intensities:  $^{101}\text{Rh}^g$

The 97.5, 114.8, and 307 keV gamma transitions were not observed, though we were unable to determine upper intensity limits below the intensities given by SPN. Kistner and Schwarzschild<sup>3</sup> observed a 114.8 keV gamma transition deexciting the 422 keV level with a branching ratio relative to the 295 keV gamma transition equal to 1/30 in disagreement with the branching ratio 1/10 determined by SPN. We quote Kistner's result in the decay scheme. The 97.5 keV gamma transition was not observed by Kistner and Schwarzschild; thus, we do not include this transition in the decay scheme.

V. DISCUSSION AND CONCLUSION

There are few theoretical calculations of the  $^{101}\text{Ru}$  positive-parity levels. Bhattacharaya and Basu<sup>29</sup> calculate energy levels and transition probabilities in the phonon plus quasi-particle model with intermediate coupling (QPC). Imanishi *et al.*<sup>30</sup> calculate the energy spectra in the rotational model with Coriolis coupling. Alzner *et al.*<sup>9</sup> calculate magnetic dipole and electric quadrupole

moments in the particle-core weak coupling limit.

Bhattacharaya and Basu utilize particle occupation probabilities that imply 19 neutrons in the valence shell  $50 < N < 82$ , nine of them in the positive parity states, in disagreement with the  $^{101}\text{Ru}$  neutron number, 57. Imanishi *et al.* did not calculate the electromagnetic transition probabilities, which prevents a more detailed test of their model. The calculation of Alzner *et al.* is very simple but shows good agreement. We will also reinforce the point of view that it is possible to understand qualitatively the positive parity levels as quasi-particles coupled to phonons.

Table IV lists all known  $^{101}\text{Ru}$  positive parity levels up to an excitation energy of 720 keV (Refs. 20, 2, 19, and this work) with the spectroscopic factors measured in the  $^{100}\text{Ru}(d,p)^{101}\text{Ru}$ . For some levels, we assign the quantum number  $J$ —quasi-particle angular momentum— and  $n, R$ —phonon number and core state angular momentum, respectively. The  $j = \frac{5}{2}$  quasi-particle coupled to one-phonon multiplet has an energy centroid of 506 keV, in agreement with the first  $2^+$  states in  $^{100}\text{Ru}$  and  $^{102}\text{Ru}$  at 540 and 475 keV, respectively.

The experimental electric quadrupole transition probabilities [ $B(E2)$ ] in  $^{101}\text{Ru}$  are given in Table V and show

TABLE V. Electric quadrupole reduced probability transition,  $B(E2)$ , in  $^{101}\text{Ru}$ . All branching ratios utilized in the preparation of this table were taken from this work. The half-lives were taken from Harmatz (Ref. 20). Energies are in keV.

Initial level energy	$I^\pi$	Final level energy	$I^\pi$	Transition energy	$B(E2)$ $e^2\text{fm}^4$
127	$\frac{3}{2}^+$	0	$\frac{5}{2}^+$	127	560(60) <sup>a</sup>
307	$\frac{7}{2}^+$	127	$\frac{3}{2}^+$	180	360(90) <sup>b</sup>
		0	$\frac{5}{2}^+$	307	50(15) <sup>a</sup>
311	$\frac{5}{2}^+$	0	$\frac{5}{2}^+$	311	200(30) <sup>a</sup>
325	$\frac{1}{2}^+$	127	$\frac{3}{2}^+$	198	< 75 <sup>b</sup>
		0	$\frac{5}{2}^+$	325	130(20) <sup>d</sup>
422	$\frac{3}{2}^+$	311	$\frac{5}{2}^+$	111	< 10 <sup>6b</sup>
		127	$\frac{3}{2}^+$	295	< 10 <sup>5b</sup>
		0	$\frac{5}{2}^+$	422	260(30) <sup>b</sup>
545	$\frac{7}{2}^+$	127	$\frac{3}{2}^+$	418	26(10) <sup>b</sup>
		0	$\frac{5}{2}^+$	545	1050(80) <sup>a</sup>
616	$(\frac{5}{2}^+)$	0	$\frac{5}{2}^+$	616	120(20) <sup>a</sup>
623	$\frac{1}{2}^+$	0	$\frac{5}{2}^+$	623	210(60) <sup>a</sup>
720	$\frac{9}{2}^+$	545	$\frac{7}{2}^+$	175	< 2 × 10 <sup>5c</sup>
		311	$\frac{5}{2}^+$	409	< 10 <sup>3c</sup>
		307	$\frac{7}{2}^+$	413	900(300) <sup>c</sup>
		0	$\frac{5}{2}^+$	720	610(50) <sup>a</sup>

<sup>a</sup>From Kistner *et al.* (Ref. 3).

<sup>b</sup>From Harmatz (Ref. 20).

<sup>c</sup>From Kajrys *et al.* (Ref. 19).

<sup>d</sup>Average from the works of Kistner *et al.* (Ref. 3) and Kajrys *et al.* (Ref. 19).

additional evidence for the assignments in Table IV. We point out that the  $B(E2)$  between states with one phonon coupled to a  $J = \frac{5}{2}$  quasi-particle and the ground state— $J = \frac{5}{2}$ , no phonon—are greatly enhanced relative to the single-particle estimate,  $28 e^2 \text{fm}^4$ . The only intramultiplet  $B(E2)$  known, from the 545 keV level to the 127 keV level, is of the order of one Weisskopf unit. Also, the  $B(E2)$  for transitions between the quasi-particle states ( $J = \frac{7}{2}$  or  $J = \frac{1}{2}$ , no phonon) and the ground state are of the order of a few Weisskopf units.

A calculation with the QPC model similar to the calculation of Bhattacharaya and Basu,<sup>29</sup> failed to explain the energy spectra, though it is able to explain most of the experimental  $B(E2)$  and spectroscopic factors.<sup>31</sup> This conforms well with the possibility of qualitative interpretation of the spectrum in the weak coupling limit. In particular, the QPC model does not explain the lowering of the  $\frac{3}{2}^+$  and  $\frac{5}{2}^+$  states assigned to a single phonon coupled to a  $J = \frac{5}{2}$  quasi-particle multiplet. The favoring of the  $\frac{3}{2}^+$  state may be understood, however, with the  $J - 1$  rule. When the  $J$  subshell is half-filled, one must correct for the Pauli principle violation in the core plus particle product state. This correction favors the state of angular momentum equal to  $J - 1$ .<sup>32-35</sup> The perturbative calcula-

tion of the energy change up to second order in the particle-phonon interaction, however, also does not lead to good agreement with experimental data<sup>31</sup> though the energy changes of the multiplet members are in the correct direction except for the  $J = \frac{5}{2}$  state.

In conclusion, the data obtained resulted in a simplification in the  $^{101}\text{Ru}$  spectrum. We suggest that the  $^{101}\text{Ru}$  for low energy excitation may be understood at least qualitatively in the general systematics of the vibrational nuclei.

#### ACKNOWLEDGMENTS

The authors would like to express their thanks to Prof. I. D. Goldman for his suggestions and continuous interest and encouragement during this work. We wish to express our gratitude to Prof. Max Cohenca, Prof. Paulo R. Pascholati, Prof. J. Takahashi, and Prof. P. Gouffon for their assistance in this experiment. We appreciate the help of Prof. F. Krmpotic in the elucidation of theoretical aspects of this work. We are grateful to Prof. W. A. Seale for his critical reading and many suggestions in the preparation of the article. The work of A.P. and A.M.P.P. was partially supported by Conselho Nacional de Pesquisas.

- 
- <sup>1</sup>C. L. Hollas, K. A. Aniol, D. W. Gebbie, M. Borsaru, I. Nurzynski, and L. O. Barbopoulos, Nucl. Phys. **A276**, 1 (1977).  
<sup>2</sup>J. L. M. Duarte, M.Sc. thesis, Instituto de Física da USP, São Paulo, Brazil, 1980.  
<sup>3</sup>O. C. Kistner and A. Schwarzschild, Phys. Rev. **154**, 1182 (1967).  
<sup>4</sup>R. B. Begzhanov, D. A. Gladyshev, K. Sh. Azimov, M. Narzikulov, and K. T. Teshabaev, Izv. Vyssh. Uchebn. Zaved. Fiz. **16**, No. 9, 82 (1973) [Sov. Phys. J. **16**, 1258 (1973)].  
<sup>5</sup>K. I. Erokhina, J. Kh. Lemberg, A. S. Mishin, and A. A. Pasternak, Izv. Akad. Nauk. SSSR, Ser. Fiz. **38**, 1673 (1974) [Bull. Acad. Sci. USSR Phys. Ser. **38**, No. 8, 97 (1974)].  
<sup>6</sup>H. Bartsch, K. Huber, U. Kneissl, and H. Krieger, Z. Phys. A **285**, 273 (1978).  
<sup>7</sup>K. Auerbach, K. Siepe, J. Wittkemper, and H. J. Korner, Phys. Lett. **23**, 367 (1966).  
<sup>8</sup>S. Buttgenbach, R. Dicke, H. Gebauer, and M. Herschel, Z. Phys. A **280**, 217 (1977).  
<sup>9</sup>A. Alzner, E. Bodenstedt, G. Gemünden, C. Hermann, H. Münnig, H. Reif, H. J. Rudolph, R. Vianden, and U. Wrede, Z. Phys. A **317**, 107 (1984).  
<sup>10</sup>J. S. Evans and R. A. Naumann, Phys. Rev. **140**, B559 (1965).  
<sup>11</sup>N. K. Aras, G. D. O'Kelley, and G. Chilosi, Phys. Rev. **146**, 869 (1966).  
<sup>12</sup>N. K. Aras, P. Fettweis, G. Chilosi, and G. D. O'Kelley, Nucl. Phys. **A169**, 209 (1971).  
<sup>13</sup>J. Sieniawski, H. Pettersson, and B. Nyman, Z. Phys. **245**, 81 (1971).  
<sup>14</sup>W. B. Cook and M. W. Johns, Can. J. Phys. **50**, 1511 (1972).  
<sup>15</sup>W. B. Cook and M. W. Johns, Can. J. Phys. **50**, 1957 (1972).  
<sup>16</sup>J. F. Wright, W. L. Talbert, Jr., and A. F. Voigt, Phys. Rev. C **12**, 572 (1975).  
<sup>17</sup>C. M. Lederer, J. M. Jaklevic, and J. M. Hollander, Nucl. Phys. **A169**, 489 (1971).  
<sup>18</sup>W. Klamra, K. Fransson, B. Sundstrom, M. Brenner, S. Engman, and R. Kvarnstrom, Nucl. Phys. **A376**, 463 (1982).  
<sup>19</sup>G. Kajrys, R. Lecomte, S. Landsberg, and S. Monaro, Phys. Rev. C **28**, 1504 (1983).  
<sup>20</sup>B. Harmatz, Nucl. Data Sheets **28**, 343 (1979).  
<sup>21</sup>P. de Gelder, D. de Frenne, and E. Jacobs, Nucl. Data Sheets **35**, 443 (1982).  
<sup>22</sup>K. Hisatake, S. Matsuo, and H. Kawakami, J. Phys. Soc. Jpn. **20**, 1107 (1965).  
<sup>23</sup>G. T. Wood, S. Koicki, and A. Koicki, Phys. Rev. **150**, 956 (1966).  
<sup>24</sup>A. V. Aldushchenkov, M. A. Voinova, V. G. Dubro, A. I. Egorov, Y. V. Kalichenev, D. M. Kaminker, L. K. Peter, and A. G. Sergeev, Izv. Akad. Nauk. SSSR, Ser. Fiz. **37**, 965 (1973) [Bull. Acad. Sci. USSR, Phys. Ser. **37**, No. 5, 48, (1974)].  
<sup>25</sup>S. Rösler, H. M. Fries, K. Alder, and H. C. Pauli, At. Data Nucl. Data Tables **21**, 91 (1978).  
<sup>26</sup>O. A. M. Helene, Nucl. Instrum. Methods **212**, 319 (1983).  
<sup>27</sup>P. Gouffon, Program IDEFIX, user manual. Documentation of the Linear Accelerator Laboratory PDP11/45 programs, Instituto de Física da USP, São Paulo, Brazil, 1983 (unpublished).  
<sup>28</sup>N. B. Gove and M. J. Martin, Nucl. Data Tables **10**, 205 (1971).  
<sup>29</sup>S. Bhattacharaya and S. K. Basu, Phys. Rev. C **18**, 2765 (1978).  
<sup>30</sup>N. Imanishi, I. Fujiwara, and T. Neshi, Nucl. Phys. **A205**, 531 (1973).  
<sup>31</sup>V. R. Vanin, Ph.D. thesis, Instituto de Física da USP, São



- Paulo, Brazil, 1984.
- <sup>32</sup>D. Bes, in *Problems of Vibrational Nuclei*, edited by G. Alaga, V. Paar, and L. Sips, (North-Holland, Amsterdam, 1975), p. 1–14.
- <sup>33</sup>A. Bohr and B. R. Mottelson, *Nuclear Structure* (Benjamin, New York, 1975), Vol. II.
- <sup>34</sup>A. Kuriyama, T. Marumori, K. Matsuyanagi, and R. Okamoto, *Prog. Theor. Phys. Suppl.* **58**, 103 (1975).
- <sup>35</sup>A. Kuriyama, T. Marumori, K. Matsuyanagi, and R. Okamoto, *Prog. Theor. Phys. Suppl.* **58**, 53 (1975).